Vol 466|22 July 2010|doi:10.1038/nature09274

LETTERS

Lunar apatite with terrestrial volatile abundances

Jeremy W. Boyce[1,2], Yang Liu[3], George R. Rossman[1], Yunbin Guan[1], John M. Eiler[1], Edward M. Stolper[1] & Lawrence A. Taylor[3]

The Moon is thought to be depleted relative to the Earth in volatile elements such as H, Cl and the alkalis[1–3]. Nevertheless, evidence for lunar explosive volcanism[4,5] has been used to infer that some lunar magmas exsolved a CO-rich and CO_2-rich vapour phase before or during eruption[6–8]. Although there is also evidence for other volatile species on glass spherules[9], until recently[10] there had been no unambiguous reports of indigenous H in lunar rocks. Here we report quantitative ion microprobe measurements of late-stage apatite from lunar basalt 14053 that document concentrations of H, Cl and S that are indistinguishable from apatites in common terrestrial igneous rocks. These volatile contents could reflect post-magmatic metamorphic volatile addition or growth from a late-stage, interstitial, sulphide-saturated melt that contained ~1,600 parts per million H_2O and ~3,500 parts per million Cl. Both metamorphic and igneous models of apatite formation suggest a volatile inventory for at least some lunar materials that is similar to comparable terrestrial materials. One possible implication is that portions of the lunar mantle or crust are more volatile-rich than previously thought.

The recent report of low but non-zero H, F, Cl and S contents of lunar glass spherules[10] has been interpreted as evidence of pre-eruptive H_2O contents as high as ~750 p.p.m., ~98% of which was lost by degassing during eruption. Estimates of the pre-eruptive Cl contents of these spherules are low (0.4 p.p.m.), implying that H_2O/Cl (by weight) ≈ 1,900—much higher than measured terrestrial melt inclusions, 95% of which have H_2O/Cl < 85 (ref. 11). These results are so important for understanding lunar origin and evolution that confirmation using an independent approach is essential. Here we provide an independent constraint on the volatile contents of lunar igneous rocks by measuring H, Cl and S contents of apatites in lunar basalt 14053 using secondary ion mass spectrometry (SIMS).

The mineral apatite—$Ca_5(PO_4)_3(F,Cl,OH)$—is widely distributed in planetary materials. Terrestrial igneous apatite incorporates S as sulphate and C as carbonate, both substituting for phosphate[12]. Terrestrial apatite is more retentive of these elements than are silicate melts or glasses[13,14], and it is therefore able to preserve magmatic volatile contents in volcanic rocks in which glasses are largely degassed[15,16]. Indirect evidence for H in lunar apatites was first observed about 40 years ago[17], and recent reports of H in lunar apatite support this hypothesis[18–20].

The Apollo 14 lunar sample 14053 is a high-Al basalt rich in K, rare-earth elements and P (KREEP), consisting dominantly of augite and plagioclase with lesser ilmenite, chromite-ulvöspinel, tridymite, Fe-Ni metal, and mesostasis containing fayalitic olivine, troilite, K-Ba-rich glass, K-feldspar, F-Cl-bearing apatite, merrillite and baddeleyite[21]. Fayalite in 14053 was partially reduced to SiO_2 + Fe metal by a subsolidus metamorphic reaction under highly reducing conditions[21]; this reaction is more pronounced near the exterior of the rock. The reductant that facilitated this reaction is inferred to have been H implanted by the solar wind, which had higher concentrations near the exterior of the rock. This metamorphic event has been interpreted as due to a post-magmatic impact and subsequent burial by hot ejecta[21]. The subsolidus reduction of fayalite is texturally associated with anhedral apatite having variable Cl and rare-earth-element contents, and it is sometimes associated with merrillite. The sample used in this study (14053,241) was from the interior of the rock where the amount of reduction is lowest, and <1 vol.% fayalite was reduced (preferentially along cracks) in the section we investigated (Fig. 1). Apatite analysed here is not visibly associated with merrillite.

Measurements of H, C, S and Cl were made using Caltech's Cameca ims 7f-GEO secondary ion mass spectrometer (see Supplementary Information). Seven analyses were made on a single, subhedral apatite crystal (Fig. 1). These analyses yielded a range of apparent H contents from 1,550 ± 110 p.p.m. H_2O to 2,405 ± 180 p.p.m. H_2O (2σ error; Fig. 2a), with an observed correlation of $^{12}C^-/^{18}O^-$ and $^{16}O^1H^-/^{18}O^-$ (correlation coefficient $R^2 = 0.76$). Analyses in an adjacent olivine crystal also yielded a positive trend but with a zero-carbon intercept within uncertainty of 0 p.p.m. H_2O, as expected for this nominally anhydrous phase. We interpret these trends as mixing lines between a carbon-poor mineral (that is, apatite in Fig. 2a) and a H- and C-bearing contaminant of unknown origin. By this interpretation, the minimum H_2O content of uncontaminated apatite is given by the intercept of a line fitted through the correlation between $^{12}C^-/^{18}O^-$ and $^{16}O^1H^-/^{18}O^-$,

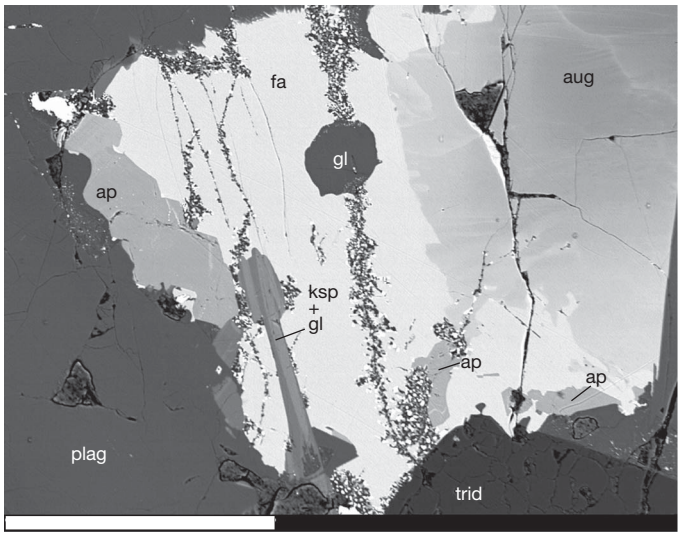

Figure 1 | Backscattered electron image of the area in rock section (14053,241) analysed in this study. Scale bar is 200 μm. Minerals are labelled as: ap (apatite), fa (fayalite), gl (glass), aug (augite), trid (tridymite), ksp (K-feldspar) and plag (plagioclase).

[1]Division of Geological and Planetary Sciences, California Institute of Technology, Pasadena, California 91125-2500, USA. [2]Department of Earth and Space Sciences, University of California, Los Angeles, California 90095-1567, USA. [3]Planetary Geosciences Institute, Department of Earth and Planetary Sciences, University of Tennessee, Knoxville, Tennessee 37996, USA.

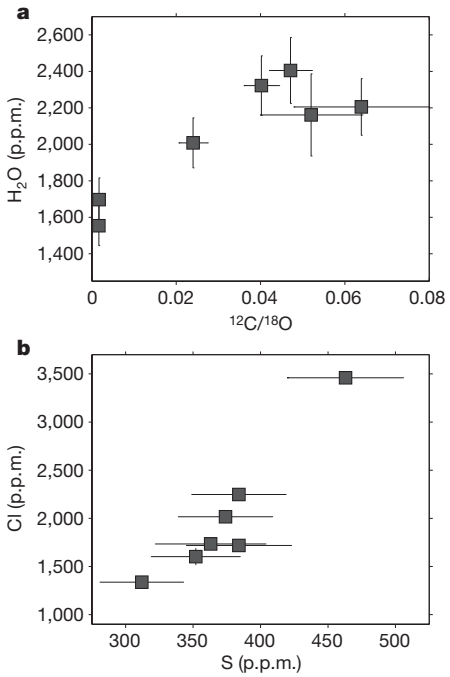

Figure 2 | Plots of H_2O versus C and Cl versus S for analyses of 14053 apatite. **a**, H_2O versus C (as ions normalized to $^{18}O^-$). **b**, Cl versus S. All concentrations are reported by weight, with hydrogen reported as H_2O and sulphur reported as S. All uncertainties are two standard deviations of the mean, with error bars also representing 2σ uncertainties, including error in calibration curves.

which corresponds to ~1,600 p.p.m. H_2O. If some of the carbon measured in apatite is structural, then the true H content of the spots with non-zero carbon would be higher than this minimum value. The minimum value of ~1,600 p.p.m. is higher than the range of concentrations measured for apatite in other sections of 14053 (~800 to ~1,000 p.p.m. H_2O; ref. 19).

Measured S and Cl abundances are not correlated with C and H abundances, suggesting that they are not dominated by hydrocarbon contamination. The seven analyses range from 310 ± 30 to 460 ± 40 p.p.m. S, and $1{,}340 \pm 45$ to $3{,}460 \pm 51$ p.p.m. Cl. The S and Cl contents in this grain are positively correlated ($R^2 = 0.90$, Fig. 2b), and their variations exceed analytical uncertainty (~4% for S and ~3% for Cl; values are 2σ). This could represent variations during magmatic growth or a post-crystallization exchange of both elements. The Cl concentrations observed in this apatite are within the much larger range of previous measurements of Cl in 14053 apatites made by electron microprobe from <0.03 to 1.57 wt% Cl (ref. 21).

Volatile abundances in apatite from lunar basalt 14053 are within the ranges of S, Cl and H abundances of apatites from terrestrial volcanic rocks[11,15,22–24]. The H in apatite from 14053 is comparable to the H content at the peak of the distribution of terrestrial apatites from mafic extrusive rocks (~1,500 p.p.m.; Fig. 3a), while the Cl content of this lunar apatite ranges from 20% to 50% of the mode of the distribution for mafic terrestrial igneous rocks (~6,500 p.p.m. Cl; Fig. 3b). S concentrations in 14053 are near the peak of the distribution of S contents measured for terrestrial mafic igneous apatites (~300–400 p.p.m. S; Fig. 3c). This comparison represents the key result of this report: apatites from lunar basalt 14053 are very similar to apatites from comparable terrestrial igneous rocks in their abundances of the volatile elements H, Cl and S.

The subsolidus reduction observed in lunar basalt 14053 has been interpreted as being due to reaction between minerals and implanted solar wind hydrogen[21]. One possibility then is that some or all of the H in the apatite we analysed was derived from H_2O formed by this reaction. The solar wind has a very low deuterium/hydrogen ratio ($D/H < 3 \times 10^{-6}$; ref. 25), so such a component would be manifested by an anomalously low D/H. Recently determined D/H of apatite in exterior sections of lunar basalt 14053 yield $D/H \approx 1.3 \times 10^{-4}$, much lower than that of other lunar apatites ($\geq 3 \times 10^{-4}$)[19]. It is thus plausible that some of the H in the apatite we analysed was incorporated from solar-wind H mobilized during the metamorphic event that reduced fayalite. Assuming a lower limit of 3×10^{-4} for the D/H of indigenous lunar hydrogen, this would imply that at least half of the H in the apatites from other sections of 14053 is derived from the solar wind[19]. The hypothesis that the H_2O in the apatite in this section of 14053 is at least partly, and perhaps largely, a subsolidus, metasomatic feature cannot be proved or disproved at this point. The apparent decoupling of the H_2O content of the apatite from the co-varying S and Cl contents is consistent with this hypothesis.

An alternative hypothesis is that the volatile contents of apatite in 14053 were set by crystallization from late-stage interstitial liquid and were largely resistant to overprinting by the later, reducing subsolidus metamorphic event. If so, then the apatite analyses reported here can be used to infer the volatile contents of the late-stage melts in 14053. This possibility is consistent with the evidence for limited subsolidus reduction in the particular section we examined. In addition, a solar-wind component is unlikely to account for the Cl or S contents of apatites in this section because Cl and S are more than three orders of magnitude less abundant in the solar wind than is H (ref. 26).

A rigorous interpretation of our data as constraints on the volatile contents of the interstitial liquid from which apatite in sample 14053 crystallized (assuming they record equilibrium between such a liquid and the apatite) would require thermodynamic models for the apatite and coexisting silicate liquid found in 14053. Unfortunately, available experimental constraints on apatite saturation in silicate melts are inadequate for such a rigorous treatment. In the absence of rigorous models of apatite thermochemistry, we have estimated the volatile content of silicate melt that could coexist with 14053 apatite using available partition coefficients between apatite and basaltic melt. (Partition coefficient D_X is defined as the mass concentration

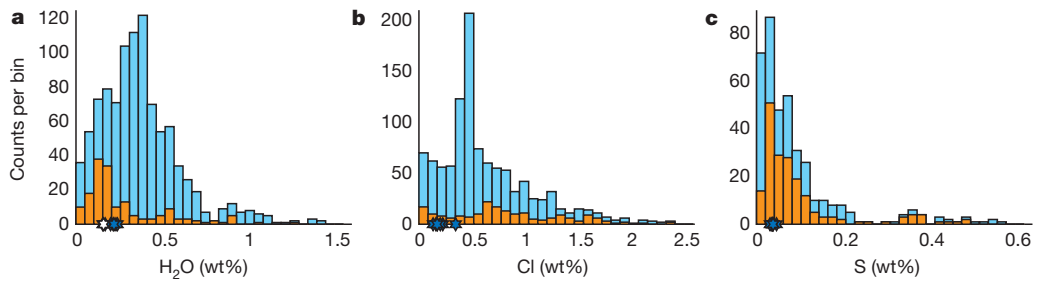

Figure 3 | Histograms of H_2O, Cl and S concentrations for terrestrial igneous apatites[11,15,22–24]. **a**, $n = 3$ for $H_2O > 1.5$; **b**, $n = 26$ for $Cl > 2.5$; **c**, $n = 8$ for $S > 0.6$. Blue bars represent terrestrial igneous apatite ($n = 976$). Orange bars represent a subset ($n = 167$) of apatite from mafic extrusive lithologies. Most of the H_2O values from the literature are calculated by difference. Lunar compositions reported from this study are marked with blue stars; a zero-carbon lunar apatite is marked with a white star.

of element X in apatite divided by the concentration of X in the melt.) We emphasize that this requires use of these partition coefficients beyond the conditions for which they have been determined experimentally and thus that this represents, at best, only a rough estimate. D_H and D_{Cl} were taken from experiments[27] in which apatite coexists with Cl^--bearing and H_2O-bearing terrestrial basaltic melts under conditions relevant to terrestrial petrogenesis. Application of the mean value of D_H from those experiments ($D_H = 0.4$) would suggest ~4,000 p.p.m. H_2O in this late-stage melt. The mean value of $D_{Cl} = 1.0$ would likewise suggest ~3,500 p.p.m. Cl in the late-stage melt; applying the same D_{Cl} approach to previously published electron probe data on apatite from 14053 would yield concentrations from within error of zero to 1.6 wt% Cl in the melt[21]. For S, we lack partitioning data at appropriately reduced conditions, but given the low sulphate content in silicate liquids at the reducing conditions relevant to crystallization of lunar basalts[3], the non-zero S content of these apatites is difficult to reconcile with the incorporation of S into apatite only as sulphate. One possibility is that a sulphide substitution into the F-Cl-OH site in apatite may occur under these conditions[28]. Evidence for a coexisting sulphide liquid in 14053 indicates that the melt was sulphide-saturated[21] and suggests S concentrations in the coexisting late-stage silicate melt from which the apatite crystallized of 1,500–3,400 p.p.m. S provided this liquid was basaltic[3].

We note that we have only estimated the volatile contents of the late-stage melt in 14053, which was residual to nearly complete crystallization of the rock and thus would have significantly concentrated incompatible elements such as H, Cl and S: of greater importance is the implied composition of the parental liquid to 14053. If we assume the relatively simple case of differentiation through fractional crystallization alone, a melt with a composition similar to the one we estimate to have been in equilibrium with 14053 apatite could be produced by 95% crystallization of anhydrous minerals from an original, primitive melt with 100–200 p.p.m. H_2O, 100–170 p.p.m. Cl, and 75–170 p.p.m. S. Although these values are strongly dependent on the assumed amount of crystallization (which is poorly constrained), these estimated H and S concentrations are of a similar order of magnitude to previous estimates for primitive lunar melts based on analyses of volcanic glass spherules[10]. However, our calculated Cl value for the primitive melt is two to three orders of magnitude higher than that estimated for the undegassed parent melt of lunar volcanic glass spherules[10]. The estimates based on apatite or spherule composition are all lower limits because these magmas may have degassed before or during apatite crystallization or spherule formation.

The observation that the H, Cl and S contents of apatite from a lunar basalt are essentially indistinguishable from apatites grown from terrestrial magmas (Fig. 3) is the key result of this study. This resemblance could be a coincidence, given the clear evidence for a metamorphic overprint in 14053. However, if the volatile contents of 14053 apatite preserve magmatic values, then our results are consistent with recent evidence that some lunar magmas contain hundreds of p.p.m. or more H_2O (ref. 10), similar to some terrestrial magmas derived by partial melting of the Earth's upper mantle[29]. One difference between estimated volatile contents of lunar magmas based on our apatite results and those based on the study of lunar glass spherules is that our results would suggest Cl contents over 200 times higher than those based on glass spherules[10] and H/Cl ratios comparable to terrestrial values. Given the KREEP-rich nature of 14053, enrichment in H, Cl and S in its source might—in hindsight—not be unexpected. Measurements of apatites from a range lunar rock types have the potential to clarify the generality and significance of the terrestrial-like H, Cl and S contents of apatite from this KREEP-rich sample.

METHODS SUMMARY

Lunar rock samples were mounted in indium with two synthetic apatites (F- and Cl- apatites with near end-member compositions) and natural apatites from the Cerro de Mercado mine in Durango, Mexico, and from Mud Tank in the Northwest Territory, Australia. The samples were given a ~90-nm-thick gold coating (three times normal), to improve electrical conductivity.

Spot analyses of C, H, F, S and Cl were made using the Cameca ims 7f-GEO at Caltech over the course of two days, and a 5-nA, 10-keV Cs^+ primary beam with normal-incidence electron gun charge compensation and 20-keV impact energy. Samples were pre-sputtered for a minimum of ~5 min before analyses. The ~20-μm beam was rastered over a 20 μm × 20 μm area. To eliminate contamination from the crater edges, a field aperture limiting the analyses to ions from the central ~10 μm of the beam and an electronic gate of 40% were used during measurements.

The following ions were measured: $^{12}C^-$, $^{16}O^1H^-$, $^{18}O^-$, $^{19}F^-$, $^{31}P^-$, $^{32}S^-$, $^{35}Cl^-$ and $^{19}F^{16}O^-$, with $^{18}O^-$ serving as the reference mass. The mass resolution obtained ($M/\Delta M \approx 5{,}700$) was sufficient to separate $^{16}O^1H^-$ from $^{17}O^-$, $^{31}P^1H^-$ from $^{32}S^-$, and $^{19}F^{16}O^-$ from $^{35}Cl^-$.

All measurements were made on a single subhedral, polycrystalline apatite grain in the larger of the two pieces of sample 14053. The grain was visible in reflected light in the SIMS, and was imaged using ^{31}P. Maps of ^{12}C were also used to place spots in judicious locations to minimize contamination, which was observed as linear streaks of high ^{12}C counts within the crystal.

Full Methods and any associated references are available in the online version of the paper at www.nature.com/nature.

Received 11 March; accepted 16 June 2010.

1. Gibson, E. K. & Moore, G. W. Volatile-rich lunar soil: evidence of possible cometary impact. *Science* **179,** 69–71 (1973).
2. Epstein, S. & Taylor, H. P. The isotopic composition and concentration of water, hydrogen, and carbon in some Apollo 15 and 16 soils and in the Apollo 17 orange soil. *4th Lunar Sci. Conf.* **2,** 1559–1575 (1973).
3. Wieczorek, M. A. *et al.* The constitution and structure of the lunar interior. *Rev. Mineral. Geochem.* **60,** 221–364 (2006).
4. McGetchin, T. R. & Head, J. W. Lunar cinder cones. *Science* **180,** 68–71 (1973).
5. Fogel, R. A. & Rutherford, M. J. Magmatic volatiles in primitive lunar glasses. I. FTIR and EPMA analyses of Apollo 15 green and yellow glasses and revision of the volatile-assisted fire-fountain theory. *Geochim. Cosmochim. Acta* **59,** 201–215 (1995).
6. Wilson, L. & Head, J. W. Deep generation of magmatic gas on the Moon and implications for pyroclastic eruptions. *Geophys. Res. Lett.* **30,** 71–74 (2003).
7. Sato, M. The driving mechanism of lunar pyroclastic eruptions inferred from the oxygen fugacity behavior of Apollo 17 orange glass. *10th Lunar Planet. Sci. Conf.* 311–325 (1979).
8. Rutherford, M. J. & Papale, P. Origin of basalt fire-fountain eruptions on Earth versus the Moon. *Geology* **37,** 219–222 (2009).
9. Delano, J. Pristine lunar glasses: criteria, data, and implications. *16th Lunar Planet. Sci. Conf.* D201–213 (1986).
10. Saal, A. E. *et al.* Volatile content of lunar volcanic glasses and the presence of water in the Moon's interior. *Nature* **454,** 192–195 (2008).
11. Sarbas, B. & Nohl, U. in *Geoinformatics 2008 — Data to Knowledge* (eds Brady, S. R., Sinha, A. K. & Gundersen, L. C.) 42–43 (Report 2008-5172, Proceedings of USGS Scientific Investigations, 2008).
12. Pan, Y. M. & Fleet, M. E. Compositions of the apatite-group minerals: substitution mechanisms and controlling factors. *Rev. Mineral. Geochem.* **48,** 13–49 (2002).
13. Brenan, J. Kinetics of fluorine, chlorine, and hydroxyl exchange in fluorapatite. *Chem. Geol.* **110,** 195–210 (1993).
14. Streck, M. J. & Dilles, J. H. Sulfur evolution of oxidized arc magmas as recorded in apatite from a porphyry copper batholith. *Geology* **26,** 523–526 (1998).
15. Boyce, J. W. & Hervig, R. L. Magmatic degassing histories from apatite volatile stratigraphy. *Geology* **36,** doi:10.1130/G24184A.1 (2008).
16. Boyce, J. W. & Hervig, R. L. Apatite as a monitor of late-stage magmatic processes at Volcán Irazú, Costa Rica. *Contrib. Mineral. Petrol.* **157,** 135–145 (2009).
17. Sclar, C. B. & Bauer, J. F. On the halogen deficiency of lunar apatite. *Meteoritics* **10,** 484–485 (1975).
18. Liu, Y. *et al.* Water in lunar mare basalt: confirmation from apatite in lunar basalt 14053. *41st Lunar Planet. Sci. Conf.* 2647 (2010).
19. Greenwood, J. P. *et al.* Water in Apollo rock samples and the D/H of lunar apatite. *41st Lunar Planet. Sci. Conf.* 2439 (2010).
20. McCubbin, F. M. *et al.* Detection of structurally bound hydroxyl in apatite from Apollo mare basalt 15058,128 using TOF-SIMS. *41st Lunar Planet. Sci. Conf.* 2468 (2010).
21. Taylor, L. A., Patchen, A., Mayne, R. G. & Taylor, D.-H. The most reduced rock from the moon, Apollo 14 basalt 14053: its unique features and their origin. *Am. Mineral.* **89,** 1617–1624 (2004).
22. Imai, A. Generation and evolution of ore fluids for porphyry Cu-Au mineralization of the Santo Tomas II (Philex) deposit, Philippines. *Resour. Geol.* **52,** 71–96 (2001).
23. Imai, A. Metallogenesis of porphyry Cu deposits of the Western Luzon Arc, Philippines: K-Ar ages, SO_3 contents of microphenocrystic apatite and significance of intrusive rocks. *Resour. Geol.* **52,** 147–161 (2002).
24. Imai, A. Variation of Cl and SO_3 contents of microphenocrystic apatite in intermediate to silicic igneous rocks of Cenozoic Japanese island arcs: Implications for porphyry Cu metallogenesis in the western Pacific island arcs. *Resour. Geol.* **54,** 357–372 (2004).

25. Epstein, S. & Taylor, H. P. O18/O16, Si30/Si28, D/H, and C13/C12 ratios in lunar samples. *Proc. 2nd Lunar Sci. Conf.* **2,** 1421–1441 (1971).
26. Fleck, B. First results from SOHO. *Astrophys. Space Sci.* **258,** 57–75 (1998).
27. Mathez, E. & Webster, J. Partitioning behavior of chlorine and fluorine in the system apatite-silicate melt-fluid. *Geochim. Cosmochim. Acta* **69,** 1275–1286 (2005).
28. Henning, P., Adolfsson, E. & Grins, J. The chalcogenide phosphate apatites $Ca_{10}(PO_4)_6S$, $Sr_{10}(PO_4)_6S$, $Ba_{10}(PO_4)_6S$ and $Ca_{10}(PO_4)_6Se$. *Z. Kristallogr.* **215,** 226–230 (2000).
29. Saal, A. E., Hauri, E. H., Langmuir, C. H. & Perfit, M. Vapour undersaturation in primitive mid-ocean-ridge basalt and the volatile content of Earth's upper mantle. *Nature* **419,** 451–455 (2002).

Supplementary Information is linked to the online version of the paper at www.nature.com/nature.

Acknowledgements This work was funded by grants from NASA Cosmochemistry (NNX08AG54G to L.A.T. and NNX09AG40G to E.M.S.), the NSF (OCE-0840983 to J.W.B.) and the Moore foundation for support of the Caltech Microanalysis Center.

Author Contributions J.W.B. led the generation and interpretation of the data, and the writing of the Letter. Y.L. prepared the rock section of 14053, collected BSE and EMP data, and contributed to the data interpretation and paper writing. G.R.R. conducted the infrared analyses of the apatites used for SIMS standards, performed the necessary calibrations of the infrared data and contributed to the data interpretation and paper writing. Y.G. set up the SIMS instrument, assisted in the formulation of the analytical protocol, carried out the SIMS measurements, and assisted in data processing and discussion. J.M.E. is the director of the Caltech Center for Microanalysis, and contributed to the data analysis and paper writing. E.M.S. contributed to the data interpretation and the paper writing. L.A.T initiated the collaboration, was allocated the 14053 sample by NASA, and contributed to the data interpretation and paper writing.

Author Information Reprints and permissions information is available at www.nature.com/reprints. The authors declare no competing financial interests. Readers are welcome to comment on the online version of this article at www.nature.com/nature. Correspondence and requests for materials should be addressed to J.W.B. (jwboyce@alum.mit.edu).

METHODS

A chip of 14053,241 was polished directly on diamond-embedded polishing laps. The polished section was carbon-coated and examined in scanning electron mode using a Cameca SX-100 electron microprobe at the University of Tennessee. Scanning electron images of areas with large apatite were obtained at beam conditions of 15 keV and 20 nA. The rock chip was then polished further to remove the layer affected by the electron beams.

Lunar rock samples were mounted in indium with two synthetic apatites (F-apatite and Cl-apatite with near-endmember compositions) and natural apatites from the Cerro de Mercado mine in Durango, Mexico, and from Mud Tank in the Northwest Territory, Australia. The samples were given a ~90-nm-thick gold coating (three times normal), to improve electrical conductivity in this fractured and friable sample.

Spot analyses of C, H, F, S and Cl were made using the Cameca ims 7f-GEO at Caltech over the course of two days, and a 5-nA, 10-keV Cs^+ primary beam with normal-incidence electron gun charge compensation and 20-keV impact energy. Samples were pre-sputtered for a minimum of ~5 min before analyses. The ~20-μm beam was rastered over a 20 μm × 20 μm area. To eliminate contamination from the crater edges, a field aperture limiting the analyses to ions from the central ~10 μm of the beam and an electronic gate of 40% were used during measurements.

The following ions were measured: $^{12}C^-$, $^{16}O^1H^-$, $^{18}O^-$, $^{19}F^-$, $^{31}P^-$, $^{32}S^-$, $^{35}Cl^-$ and $^{19}F^{16}O^-$. The $^{12}C^-$ image was examined before data collection to make sure that no C-rich particles or veins were present in the analysed area. Ion $^{18}O^-$ served as the reference mass, and $^{19}F^{16}O^-$ served as an alternative analytical line for ^{19}F, which is often present in amounts that (under these conditions) exceed the preferred range of the electron multiplier. The mass resolution obtained ($M/\Delta M \approx 5{,}700$) was sufficient to separate $^{16}O^1H^-$ from $^{17}O^-$, $^{31}P^1H^-$ from $^{32}S^-$, and $^{19}F^{16}O^-$ from $^{35}Cl^-$.

All measurements were made on a single subhedral, polycrystalline apatite grain in the larger of the two pieces of sample 14053. The grain was visible in reflected light in the SIMS, and was imaged using ^{31}P. Maps of ^{12}C were also used to place spots in judicious locations to minimize contamination, which was observed as linear streaks of high ^{12}C counts within the crystal.

Seven analyses of lunar apatites were made that did not appear to be affected by charging or other analytical problems. The range of $^{16}O^1H/^{18}O$ values observed for the lunar apatite is 0.29–0.44. A range of $^{12}C/^{18}O$ values was also observed, and there exists a significant positive correlation ($R^2 = 0.76$) between $^{12}C/^{18}O$ and $^{16}O^1H/^{18}O$ as shown in Supplementary Fig. 1. This has been observed previously and is interpreted as a mixing line between a low-^{12}C, low-$^{16}O^1H$ apatite component and a high-^{12}C, high-$^{16}O^1H$ hydrocarbon (contaminant) component. If this interpretation is correct, then the intercept would be the point of zero contamination (within the framework of this two-component model). This intercept ($^{16}O^1H/^{18}O = 0.30$) is within error of the two measurements with the lowest C and H. Because of the potential for contamination in the most H-rich analyses, we will limit further discussion in this document to the zero-hydrocarbon intercept.

The most robust calibration we have for H in apatite is pinned on the manometric measurements by Nadeau *et al.*[30] of H_2O in two grains of Mud Tank apatite. The two measurements were 0.80 wt% and 0.86 wt% H_2O, from which we have taken a mean of 0.83 wt% (or 8,300 p.p.m. H_2O). From this single point (and an assumption of a zero-intercept in the infrared measurements), we are able to calibrate, using infrared spectroscopy from the sample in ref. 30, three additional secondary standards that lack independent measurement of H_2O: Two synthetic apatites (ClAp = 42 p.p.m. H_2O; FAp = 192 p.p.m. H_2O) and one natural apatite (Durango = 1,170 p.p.m. H_2O). Using these three values, we can define an H_2O calibration curve for this SIMS session (Supplementary Fig. 2). The ClAp measurements from the first day of the session (analyses A to D) are consistently higher than from the second day (when the bulk of the analyses were performed), because of a dramatic decrease in the H backgrounds. All lunar apatite analyses were performed on the second day, and only data from that same day are used for the calibration. Working with this calibration, we can now estimate the H_2O content of lunar apatites. The 'zero hydrocarbon' intercept yields a value of 1,600 p.p.m., within error of the mean of the lowest values (1,554 ± 110 and 1,697 ± 120 p.p.m. H_2O).

None of the seven analyses of sulphur appear to have been influenced by contamination, because there are no correlations with $^{12}C^-/^{18}O^-$. Measured $^{32}S/^{18}O$ values vary from 0.40 to 0.60, with a mean uncertainty from counting statistics and background corrections of about 4%. Ratios are converted to absolute concentrations with a two-point calibration curve (Supplementary Fig. 3). This curve is defined by two natural apatite crystals, the first (Durango, Mexico) with an independent measurement of S (1,480 p.p.m. S; ref. 31), and the other a secondary standard with a concentration of 34.6 ± 2.6 p.p.m. S (2σ, $N = 21$), as defined by previous SIMS analyses, relative to the Durango standard. The addition of this secondary standard does not significantly change the calibration slope (because it is defined by the value of the Durango), but is an excellent check of our ability to accurately measure small concentrations of S.

Chlorine measurements are also apparently not affected by contamination. Measured $^{35}Cl/^{18}O$ values vary from 1.3 to 3.6, with average analytical uncertainties of about 3%. These ratios correspond to concentrations ranging from 1,290–3,370 p.p.m. Cl when calibrated against synthetic chlorapatite and fluorapatite crystals (Supplementary Fig. 4). The fluorapatite is a low-Cl secondary standard (42 ± 1 p.p.m., $n = 21$ in previous SIMS sessions), the omission of which does not significantly change the calibration curve, but serves to demonstrate our ability to measure small values of Cl during this session.

Fluorine was also measured during this session, as both $^{19}F^-$ ions and $^{19}F^{16}O^-$ ions, the latter chosen to mitigate problems encountered with large count rates of $^{19}F^-$, which exceed the preferred range of the electron multiplier. However, as previously documented[15], F measurements made by SIMS in apatite typically display poor reproducibility, much worse than any other element measured, despite the large abundances in natural and synthetic apatites. This may be caused by the ease with which F is ionized, making it more susceptible than other elements to variations in both primary and secondary electron ionization. F measurements made at mass/charge = 19 often exceed the useful range of the electron multiplier under the analytical conditions useful for measuring low H contents. Measurements of fluorine using $^{19}F^{16}O^-$ ions are not reproducible (48% scatter for synthetic fluorapatite, 2σ, $n = 5$). The most robust estimate of fluorine is often obtained by assuming that F + Cl + OH = 100% (complete occupancy of that site in the crystal). It should be noted that such a calculation is inherently different than the common—yet inadvisable—practice of calculating OH in apatite by subtracting measured F and Cl. Such an estimate of a small number by subtraction of large numbers is subject to propagation of the error in the fluorine measurement which—even if small in terms of relative percentage—is often larger than the amount of OH being estimated, resulting in errors that can exceed 100%.

30. Nadeau, S. L., Epstein, S. & Stolper, E. Hydrogen and carbon abundances and isotopic ratios in apatite from alkaline intrusive complexes, with a focus on carbonatites. *Geochim. Cosmochim. Acta* **63**, 1837–1851 (1999).
31. Peng, G., Luhr, J. F. & McGee, J. J. Factors controlling sulfur concentrations in volcanic apatite. *Am. Mineral.* **82**, 1210–1224 (1997).